Guiding and thermal properties of a hybrid polymer-infused photonic crystal fiber

Christos Markos,[1,2,*] Kyriakos Vlachos,[1] and George Kakarantzas[2]

[1]*Computer Engineering and Informatics Dept. & Computer Technology Institute and Press, University of Patras, Rio, GR26500, Greece*

[2]*National Hellenic Research Foundation, Theoretical and Physical Chemistry Institute, Athens, GR11635, Greece*

**cmarkos@ceid.upatras.gr*

Abstract: In this work, we investigate the guiding properties of a hybrid polymer (poly-dimethylsiloxane)/silica photonic crystal fiber (PCF). In particular, we demonstrate how the basic guiding properties of a conventional PCF are changed due to the infusion of poly-dimethylsiloxane (PDMS) in its air-holes. We show that PDMS infiltration allows tuning of single mode operation, confinement loss, effective modal area (EMA) and numerical aperture (NA) with wavelength and/or temperature. This is primarily due to the enhancement of evanescent field interaction, lending some important characteristics for designing tunable fiber devices. Numerical calculations were performed for different relative hole sizes, d/Λ (0.35-0.75), of PCF for a 500-1700nm wavelength and 0-100°C temperature range, whereas direct comparison with a conventional air-filled PCF is also shown.

OCIS codes: (060.5295) Photonic crystal fibers; (060.4005) Microstructured fibers; (230.1150) All-optical devices; (060.2290) Fiber materials; (160.6840) Thermo-optical materials.

References and links

1. P. St. J. Russell, "Photonic crystal fibers," Science **299**(5605), 358–362 (2003).
2. J. C. Knight, T. A. Birks, P. St. J. Russell, and D. M. Atkin, "All-silica single-mode optical fiber with photonic crystal cladding," Opt. Lett. **21**(19), 1547–1549 (1996).
3. T. T. Larsen, A. Bjarklev, D. S. Hermann, and J. Broeng, "Optical devices based on liquid crystal photonic bandgap fibers," Opt. Express **11**(20), 2589–2596 (2003).
4. T. T. Alkeskjold, J. Lægsgaard, A. Bjarklev, D. Hermann, A. Anawati, J. Broeng, J. Li, and S. T. Wu, "All-optical modulation in dye-doped nematic liquid crystal photonic bandgap fibers," Opt. Express **12**(24), 5857–5871 (2004).
5. W. Yuan, L. Wei, T. T. Alkeskjold, A. Bjarklev, and O. Bang, "Thermal tunability of photonic bandgaps in liquid crystal infiltrated microstructured polymer optical fibers," Opt. Express **17**(22), 19356–19364 (2009).
6. D. C. Zografopoulos, E. E. Kriezis, and T. D. Tsiboukis, "Tunable highly birefringent bandgap-guiding liquid-crystal microstructured fibers," J. Lightwave Technol. **24**(9), 3427–3432 (2006).
7. R. T. Bise, R. S. Windeler, K. S. Kranz, C. Kerbage, B. J. Eggleton, and D. J. Trevor, "Tunable photonic band gap fiber," in Proc. Opt. Fiber Commun. Conf. (OFC), Anaheim, CA, 2002, pp. 466–468.
8. L. Rindorf, J. B. Jensen, M. Dufva, L. H. Pedersen, P. E. Høiby, and O. Bang, "Photonic crystal fiber long-period gratings for biochemical sensing," Opt. Express **14**(18), 8224–8231 (2006).
9. C. Markos, W. Yuan, K. Vlachos, G. E. Town, and O. Bang, "Label-free biosensing with high sensitivity in dual-core microstructured polymer optical fibers," Opt. Express **19**(8), 7790–7798 (2011).
10. A. Candiani, M. Konstantaki, W. Margulis, and S. Pissadakis, "A spectrally tunable microstructured optical fiber Bragg grating utilizing an infiltrated ferrofluid," Opt. Express **18**(24), 24654–24660 (2010).
11. M. Hautakorpi, M. Mattinen, and H. Ludvigsen, "Surface-plasmon-resonance sensor based on three-hole microstructured optical fiber," Opt. Express **16**(12), 8427–8432 (2008).
12. C. G. Poulton, M. A. Schmidt, G. J. Pearce, G. Kakarantzas, and P. St. J. Russell, "Numerical study of guided modes in arrays of metallic nanowires," Opt. Lett. **32**(12), 1647–1649 (2007).
13. H. W. Lee, M. A. Schmidt, H. K. Tyagi, L. P. Sempere, and P. St. J. Russell, "Polarization-dependent coupling to plasmon modes on submicron gold wire in photonic crystal fiber," Appl. Phys. Lett. **93**(11), 111102 (2008).
14. P. S. Westbrook, B. J. Eggleton, R. S. Windeler, A. Hale, T. A. Strasser, and G. L. Burdge, "Cladding-mode resonances in hybrid polymer-silica microstructured optical fiber gratings," IEEE Photon. Technol. Lett. **12**(5), 495–497 (2000).

#162526 - $15.00 USD Received 8 Feb 2012; revised 27 May 2012; accepted 16 Jun 2012; published 19 Jun 2012

15. C. Markos, K. Vlachos, and G. Kakarantzas, "Bending loss and thermo-optic effect of a hybrid PDMS/silica photonic crystal fiber," Opt. Express **18**(23), 24344–24351 (2010).
16. B. T. Kuhlmey, B. J. Eggleton, and D. K. C. Wu, "Fluid-filled solid-core photonic bandgap fibers," J. Lightwave Technol. **27**(11), 1617–1630 (2009).
17. C. Kerbage, P. Steinvurzel, P. Reyes, P. S. Westbrook, R. S. Windeler, A. Hale, and B. J. Eggleton, "Highly tunable birefringent microstructured optical fiber," Opt. Lett. **27**(10), 842–844 (2002).
18. P. Steinvurzel, B. J. Eggleton, C. M. de Sterke, and M. J. Steel, "Continuously tunable bandpass filtering using high-index inclusion microstructured optical fiber," Electron. Lett. **41**(8), 463–464 (2005).
19. C. Kerbage, A. Hale, A. Yablon, R. S. Windeler, and B. J. Eggleton, "Integrated all-fiber variable attenuator based on hybrid microstructure fiber," Appl. Phys. Lett. **79**(19), 3191–3193 (2001).
20. A. Hassani and M. Skorobogatiy, "Design of the microstructured optical fiber-based surface plasmon resonance sensors with enhanced microfluidics," Opt. Express **14**(24), 11616–11621 (2006).
21. D. K. C. Wu, B. T. Kuhlmey, and B. J. Eggleton, "Ultrasensitive photonic crystal fiber refractive index sensor," Opt. Lett. **34**(3), 322–324 (2009).
22. W. Qian, C. L. Zhao, S. He, X. Dong, S. Zhang, Z. Zhang, S. Jin, J. Guo, and H. Wei, "High-sensitivity temperature sensor based on an alcohol-filled photonic crystal fiber loop mirror," Opt. Lett. **36**(9), 1548–1550 (2011).
23. Y. Fainman, L. P. Lee, D. Psaltis, and C. Yang, *Optofluidics: Fundamentals, Devices, and Applications* (McGraw-Hill, 2010).
24. F. Schneider, J. Draheim, R. Kamberger, and U. Wallrabe, "Process and material properties of polydimethylsiloxane (PDMS) for Optical MEMS," Sens. Actuators A Phys. **151**(2), 95–99 (2009).
25. http://www.nktphotonics.com/lmafibers-specifications
26. K. Nielsen, D. Noordegraaf, T. Sorensen, A. Bjarklev, and T. P. Hansen, "Selective filling of photonic crystal fibers," J. Opt. A, Pure Appl. Opt. **7**(8), L13–L20 (2005).
27. C. P. Yu and H. C. Chang, "Yee-mesh-based finite difference eigenmode solver with PML absorbing boundary conditions for optical waveguides and photonic crystal fibers," Opt. Express **12**(25), 6165–6177 (2004).
28. Z. Zhu and T. Brown, "Full-vectorial finite-difference analysis of microstructured optical fibers," Opt. Express **10**(17), 853–864 (2002).
29. J. P. Berenger, "A perfectly matched layer for the absorption of electromagnetic waves," J. Comput. Phys. **114**(2), 185–200 (1994).
30. E. Palik, *Handbook of Optical Constants of Solids I–III* (Academic, 1998).
31. M. Nielsen and N. Mortensen, "Photonic crystal fiber design based on the V-parameter," Opt. Express **11**(21), 2762–2768 (2003).
32. N. A. Mortensen, J. R. Folkenberg, M. D. Nielsen, and K. P. Hansen, "Modal cutoff and the *V* parameter in photonic crystal fibers," Opt. Lett. **28**(20), 1879–1881 (2003).
33. J. R. Folkenberg, N. A. Mortensen, K. P. Hansen, T. P. Hansen, H. R. Simonsen, and C. Jakobsen, "Experimental investigation of cutoff phenomena in nonlinear photonic crystal fibers," Opt. Lett. **28**(20), 1882–1884 (2003).
34. T. P. White, R. C. McPhedran, C. M. de Sterke, L. C. Botten, and M. J. Steel, "Confinement losses in microstructured optical fibers," Opt. Lett. **26**(21), 1660–1662 (2001).
35. K. Petermann, "Fundamental mode micro bending loss in graded index and w fibers," Opt. Quantum Electron. **9**(2), 167–175 (1977).
36. D. Marcuse, "Loss analysis of single-mode fiber splices," Bell Syst. Tech. J. **56**, 703 (1977).
37. N. A. Mortensen, J. R. Folken, P. M. W. Skovgaard, and J. Broeng, "Numerical aperture of single-mode photonic crystal fibers," IEEE Photon. Technol. Lett. **14**(8), 1094–1096 (2002).
38. N. A. Mortensen, "Effective area of photonic crystal fibers," Opt. Express **10**(7), 341–348 (2002).
39. C. M. B. Cordeiro, M. A. R. Franco, G. Chesini, E. C. S. Barretto, R. Lwin, C. H. Brito Cruz, and M. C. J. Large, "Microstructured-core optical fiber for evanescent sensing applications," Opt. Express **14**(26), 13056–13066 (2006).
40. H. R. Sørensen, J. Canning, J. Lægsgaard, and K. Hansen, "Control of the wavelength dependent thermo-optic coefficients in structured fibers," Opt. Express **14**(14), 6428–6433 (2006).

1. Introduction

Photonic crystal fiber (often referred as microstructured or 'holey' fiber) possesses many distinguished properties and characteristics compared to conventional single mode fiber [1]. This unique kind of optical fibers constitute micrometer-scaled holes running along their entire length which usually are arranged in a hexagonal pattern [2]. This feature enables the infiltration of advanced materials and liquids such as liquid crystals [3–6], high index liquids [7], biolayers [8,9], ferrofluids [10], metals [11–13] as well as polymers [14,15], into the air-holes of the PCF. Infusion of the above mentioned different materials lends the ability to modify the guiding properties and Behaviour of these fibers develops tunable devices [16,17], filters [18], attenuators [19], sensors [20–22] etc.

#162526 - $15.00 USD Received 8 Feb 2012; revised 27 May 2012; accepted 16 Jun 2012; published 19 Jun 2012

During the last decade, polymers have also attracted a lot of scientific interest because they are flexible materials with good mechanical properties, relatively low cost, and often suitable for photonic applications [23]. Limited research has been carried out so far though on the development of polymer infused PCF-based devices. Kerbage et al. reported a highly tunable birefringent microstructured optical fiber, where the variation of the refractive index of the infused polymer allows tuning of the guiding properties [17]. The proposed device required however post-processing (tapering) for increasing the interaction of the evanescent field with the infused polymer, which may result in high losses. In addition, polymers can exhibit shrinkage during polymerization and create stress and often cracks [16]. Consequently, the choice of the active polymer has a crucial role in the development of tunable devices.

A widely known and used polymer in the field of micro/optofluidics is the poly-dimethylsiloxane (PDMS). It has been used as stamp resin in the procedure of soft lithography, making it one of the most common materials used for flow delivery in microfluidics chips [23]. PDMS is a low cost material and it has very good optical and mechanical properties as well as low shrinkage and it can be fabricated very easily [23]. Its refractive index is around 1.41 and it is highly transparent to a wide range of wavelengths [24]. The combination of the unique optical properties of PDMS with the mature technology of PCFs can constitute an efficient route to development of compact cost-effectiveness tunable devices and sensors [15].

In this work, we present a detailed numerical analysis combined with experimental loss measurement of a PDMS infiltrated all-silica PCF. We demonstrate that PDMS infusion allows the tuning of basic guiding characteristics that lend many advantages, when designing tunable fiber devices. In particular, we show that PDMS infusion allows tuning single mode operation, effective modal area (EMA) and numerical aperture (NA) with wavelength and temperature as well as varying confinement loss and enhancing evanescent field interaction. These are important features for developing tunable devices (i.e. filters, sensors, tunable birefringence devices, high NA fibers, etc.) using conventional PCFs infiltrated with polymer (PDMS) materials.

The rest of the paper is organized as follows. In section 2, we experimentally measured PDMS absorption as well as the transmission losses of different PDMS–filled PCFs. Section 3 details the guiding properties (Section 3.1) as well as thermal properties (Section 3.2) of the fiber. In particular it is shown, how the infused polymer material affects the guiding mechanism of the fiber in terms of the effective index of the fundamental guiding mode (n_{eff}), effective modal area (EMA), confinement loss, numerical aperture (NA), single mode operation and fraction of power in the material-filled cladding. It is also shown how these parameters can be significantly tuned with temperature, due to the high thermo-optic coefficient of PDMS. Different relative hole sizes are employed, while results are compared with conventional (unfilled) PCFs.

2. Fiber samples preparation and loss measurements

In this section, basic absorption and loss measurements are provided to demonstrate the ease of fiber development as well as determine its loss performance. The poly-dimethylsiloxane (PDMS) was from Dow Corning (Sylgard-184) and was prepared by mixing elastomer and curing agent at 10:1 ratio [24]. For determining the absorption coefficient of PDMS, we drop casted the polymer in a glass substrate and measured the material absorption using a spectrophotometer and a step profilometer to define the film thickness of the sample. Figure 1 displays the absorption coefficient from 500-to-2000 nm wavelength spanning. At short wavelengths, the polymer exhibits a relative low absorption with only a high peak at 1186 nm and a minimum at 1320 nm. At longer wavelengths absorption coefficient increases significantly, exhibiting a maximum at ~1750nm.

#162526 - $15.00 USD Received 8 Feb 2012; revised 27 May 2012; accepted 16 Jun 2012; published 19 Jun 2012

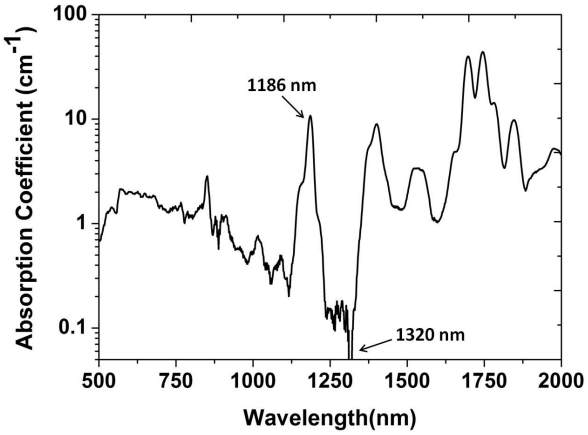

Fig. 1. Absorption coefficient of Poly-dimethylsiloxane (PDMS) material (logarithmic scale).

In our experiments, we employed four different commercially available PCFs named as LMA-13, 12-01, 10, 5, (see [25] for fiber specifications), with different d and Λ each (where d corresponds to the diameter of the cladding-hole and Λ is the pitch of the fiber). Table 1 shows the structural parameters (i.e. d and Λ) of the fibers. The fibers were infiltrated with PDMS using a custom-built pressure cell. The infiltration length depends on the viscosity of the material (in this case 3900 centipoise), the cladding-holes diameter of the fiber, and the applied pressure [26]. For example in the case of an LMA-5 fiber, applying a constant pressure of ~15 bars for 1.5 hours was enough to fill a fiber length of ~2 cm. Different samples were prepared and cured at room temperature for 48 hours according to the specifications of detailed in [24]. Figure 2(a) shows the optical microscope image of the LMA-13 filled with the polymer and Fig. 2(b) shows the scanning electron microscope (SEM) image of the same air-filled fiber.

Table 1. Structural Parameters of the Fibers

	Parameters (μm)	
Fibers	d	Λ
LMA-13	4.3	8.5
LMA-12-01	3.5	7.7
LMA-10	3.46	7.2
LMA-5	1.4	3.1

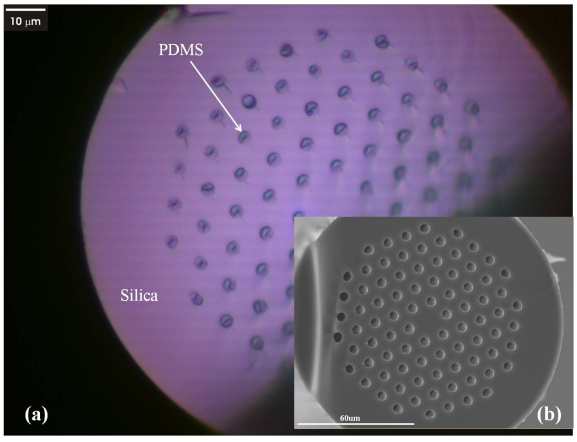

Fig. 2. (a) Optical microscope image of the PDMS-filled PCF (LMA-13). (b) SEM image of a conventional (empty) PCF fiber.

#162526 - $15.00 USD Received 8 Feb 2012; revised 27 May 2012; accepted 16 Jun 2012; published 19 Jun 2012

The loss performance of the PDMS-filled PCFs were measured using cut-back method by launching white light from a broadband supercontinuum laser source (500-1700nm). Figure 3 displays the experimental set-up. The output beam was collected with a 20 × microscope objective and a multimode fiber, while the transmitted signal was monitored on an optical spectrum analyzer. Any undesired cladding light was blocked by inserting an iris diaphragm into the beam path, such that only light from the waveguide core was recorded.

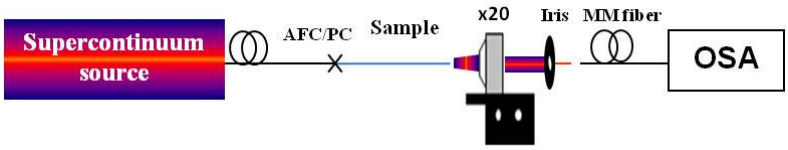

Fig. 3. Experimental set-up.

The corresponding measured losses of the polymer filled LMA-13, 12-01, 10, and 5 from 500 to 1700 nm is shown in Fig. 4. LMA-13, 12-01 and 10 have relatively large core compared to LMA-5 and therefore confinement loss is directly affecting the total loss of the fiber. Therefore, LMA-13 has higher loss than 12-01, and 10. However, it can be clearly seen that the highest values of loss obtained for the case of LMA-5 where the light-polymer interaction is the highest compared to all the other cases. The corresponding calculated fraction of power in the cladding is ~1.33% at 600 nm while for example in LMA 12-01 is ~0.09% at the same wavelength. Similarly, at longer wavelengths, i.e. 1400 nm, the fraction of power in LMA 5 is ~14% while in LMA 12-01 is ~1.9%. Due to the high absorption coefficient of PDMS at long wavelengths (higher than 1320 nm) as demonstrated in Fig. 1, combined with high confinement loss (fundamental mode starts to become a leaky mode), LMA-5 exhibits consequently very high losses at these wavelengths as shown in Fig. 4. It should be also mentioned that the loss measurement performed with great care in order to minimize errors such as in/out coupling instabilities, power fluctuation, cleaving quality, etc.

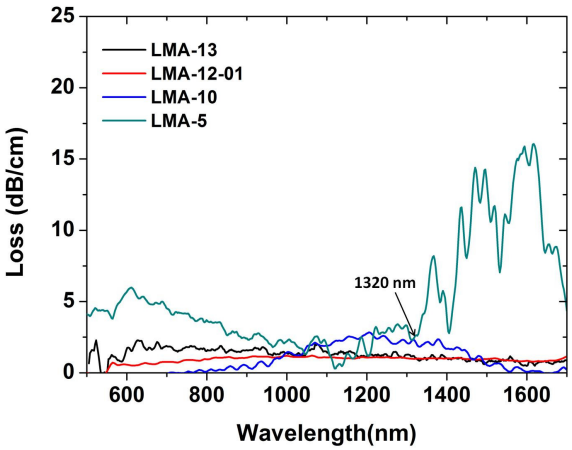

Fig. 4. Loss measurements (dB/cm) of LMA-13, 12-01, 10, and 5 from 500 to 1700 nm.

3. Numerical modeling

In our calculations we considered a standard index-guiding photonic crystal fiber with the air-holes arranged in a hexagonal array as shown in Fig. 5(a). We investigated five different structures with d/Λ = 0.35,0.45,0.55,0.65,0.75. The diameter of the cladding holes remained constant to d = 3.5 μm for all cases, which in experimental terms are big enough for the infiltration of a high viscosity polymer over several centimeters [26]. The host material of the

#162526 - $15.00 USD Received 8 Feb 2012; revised 27 May 2012; accepted 16 Jun 2012; published 19 Jun 2012

fiber was fused silica while the air-holes of the PCF were unselectively filled with PDMS. The refractive index profile of the hybrid structure is shown in Fig. 5(b).

The numerical method we employed to find out the guiding and thermal properties of the PDMS-filled PCFs is the Yee-mesh-based full-vector finite difference method [27] which is an efficient and accurate numerical mode solver for the analysis of optical waveguides and PCF structures [27,28]. In Figs. 5(c) and 5(d) we show the calculated effective indices of the fundamental guiding mode at 1550 nm wavelength of a conventional (unfilled) and PDMS filled PCF. In order to achieve accurate predictions in the numerical computation of the presented hybrid PDMS/Silica PCF cases, it is important to select the appropriate mesh spacing (grid size). With respect to the discretization scheme that was used in the calculation, reasonably accurate results can be obtained by keeping the mesh spacing at: $\lambda/15$ [27]. The boundary condition is another critical factor for simulation of mode properties. An absorbing perfectly matched layer (PML) boundary condition [29] was employed in our case for the truncation of computation domain without reflection. In all cases, we considered only the x-polarized mode since the difference between the two orthogonal polarizations was negligible.

Numerical results are divided into two sections. Section 3.1 considers the guiding properties of the hybrid PCF from 500 nm to 1700 nm wavelength. In our study, we have considered both the dispersion of fused silica and PDMS. The refractive index of silica was calculated using Palik's parameters [30], while the real part of the refractive index of PDMS using its Sellmeier equation, where the coefficients were experimentally demonstrated in [24]. The imaginary part of the refractive index was extracted based on the absorption measurements of the material (see Section 2).

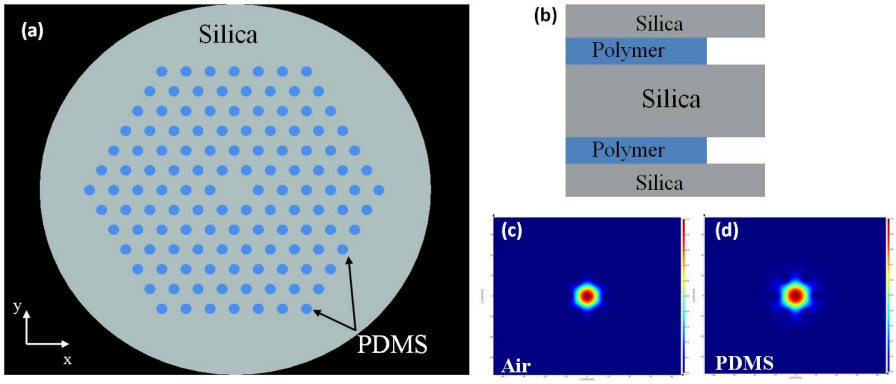

Fig. 5. (a) Hybrid polymer/silica simulated PCF. (b) Refractive index profile of the hybrid structure. Example of the calculated fundamental guiding mode profile of the PCF with d/Λ = 0.35 at 1550 nm (c) with air and (d) infused with PDMS polymer

In section 3.2 we investigate the thermal properties of the hybrid fiber. PDMS exhibits one of the highest linearly negative thermo-optic coefficient that corresponds to $dn/dT = -4.5x10^{-4}/°C$ [15]. We showed the effect of temperature in terms of effective index of the fundamental guiding mode, confinement loss, effective modal area, numerical aperture and fraction of power in the PDMS-filled holes of the PCF. Our calculations were performed at 633 nm and 1550 nm wavelength. At 633 nm, the infused polymer exhibits a relative low absorption loss, while 1550 nm is a widely used wavelength at C-band.

3.1 Guiding properties of the polymer-infused PCF

In this section, we analyze the guiding mechanism of the PDMS-filled PCF for a wavelength range of 500 nm up to 1700 nm, for different relative hole sizes, d/Λ, at room temperature. Depending on the structural dimensions of hole diameter d and pitch Λ, the fiber comprises both single- and multi-mode guidance. The V-parameter (normalized frequency) is an

#162526 - $15.00 USD Received 8 Feb 2012; revised 27 May 2012; accepted 16 Jun 2012; published 19 Jun 2012

essential factor which determines the guiding properties of the fiber. The formulation of the V-parameter for a PCF is given by [31]:

$$V - parameter = 2\pi \frac{\Lambda}{\lambda} \sqrt{n_{FM}^2(\lambda) - n_{FSM}^2(\lambda)} \quad (1)$$

Despite the fact, that this mathematical formula is similar to the expression for the standard optical fibers, the unique structure of PCF is taken into account. In Eq. (1), the term $n_{FM}^2(\lambda)$ corresponds to the effective index of the fundamental guiding mode at a particular wavelength and respectively $n_{FSM}^2(\lambda)$ corresponds to the effective index of the first cladding mode in the infinite cladding structure which is usually defined as the fundamental space filling mode. For the fully detailed analysis of this expression refer to [32].

Figure 6 shows the calculated V-parameter of the hybrid polymer/silica PCF versus wavelength operating wavelength for different d/Λ. The dashed lines correspond to the conventional unfilled PCF of the corresponding same d/Λ, while the black dashed line indicates the higher-order mode cut-off and is associated with a value of $V_{PCF} = \pi$, as demonstrated by Mortensen et al [32] and validated in [33]. From Fig. 6, it can be clearly seen that PDMS inclusion in PCF, converts a multimode fiber (see conventional air-filled PCF in Fig. 6) to endlessly single-mode according to the relative hole size d/Λ for specific wavelength ranges. This is an important feature for developing tunable fiber devices. For example, in the case of d/Λ = 0.55, the PDMS-filled PCF exhibits single mode operation above 800 nm wavelength, while the structures with d/Λ = 0.65 and 0.75 above 1100 nm and 1300 nm, respectively. The corresponding conventional unfilled PCF exhibits multimode operation across the whole wavelength span.

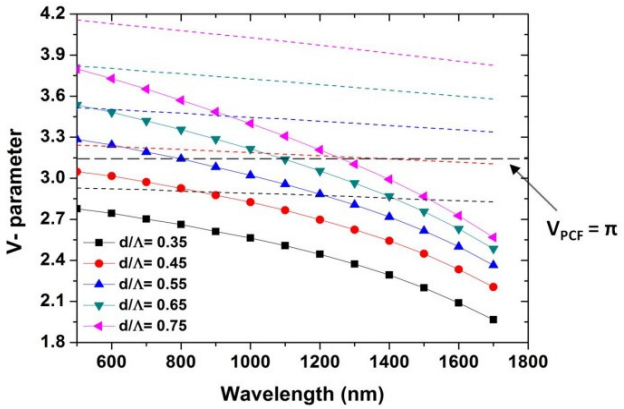

Fig. 6. Numerical calculations of the V-parameter of the PDMS filled PCF for different relative hole sizes. The dashed lines correspond to the conventional unfilled PCF. The black dashed line indicates the single-mode operation threshold.

Figure 7(a) shows the effective indices (n_{eff}) of the fundamental guided modes again for different relative-hole sizes. From Fig. 7(a), it can be seen that there is an overall increment of the effective indices of the fundamental mode of the hybrid structure (dashed lines) against conventional PCF (solid lines). This is due to the fact that the average refractive index of the cladding in the hybrid fiber is higher than the conventional one. Figure 8(b) displays the confinement loss, which is relatively low at short wavelengths but linear increases with wavelength. The confinement loss for holes sizes higher than 0.55, was negligible, since the guiding mode is highly confined to the core of the fiber.

#162526 - $15.00 USD Received 8 Feb 2012; revised 27 May 2012; accepted 16 Jun 2012; published 19 Jun 2012

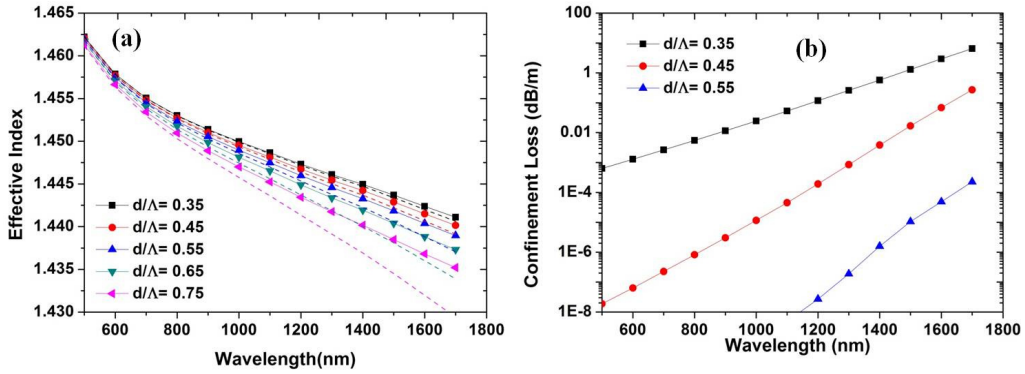

Fig. 7. (a) Effective index of the PDMS-filled PCF versus wavelength for different relative hole sizes Dashed lines correspond to the conventional (unfilled) PCF. (b) Confinement loss versus wavelength of the PDMS-filled PCF.

Another parameter of great importance is the effective modal area (EMA), as it is directly related to the confinement loss [34], micro-bending loss [35], splicing loss [36] and numerical aperture [37]. The effective area of the fiber core A_{eff} is given by [38]:

$$A_{eff} = \frac{\left(\iint_S |E_t|^2 dxdy\right)^2}{\iint_S |E_t|^4 dxdy} \tag{2}$$

In Eq. (2), the E_t is the transverse electric field vector and S denotes the cross-section of the fiber. Figure 8(a) shows the response of EMA of the hybrid (solid lines) and conventional (dashed lines) PCF. As expected, increasing the relative hole size d/Λ of the hybrid PCF, the mode becomes more confined and consequently reducing EMA. In contrast, EMA of a conventional PCF exhibits almost flat response (see black dashed line in Fig. 8(a)). Tuning EMA is of great importance for fiber laser application and the infusion of PDMS enables the ability to tune EMA based on operating wavelength as well as when varying temperature (see section 3.2). Numerical aperture, NA, is another important parameter which is directly related to the effective modal area EMA and can be expressed as:

$$\mathrm{NA} = \sin\Theta \approx (1 + \pi A_{eff} / \lambda^2)^{-1/2} \tag{3}$$

where Θ is the half divergence angle of the light radiated from the end-facet of the fiber. Figure 8(b) shows the NA change versus wavelength. It can be seen that he increase in NA is higher for higher relative hole sizes. For example, in the case of d/Λ = 0.75, NA exhibit an increase from ~0.06 to 0.15 over the 500 to 1700nm wavelength span, while only from 0.02 to 0.04 for d/Λ = 0.35. In either case, increasing NA is significantly important, especially when considering fibers for non-linear applications (e.g. supercontinuum generation) due to launching difficulties.

#162526 - $15.00 USD Received 8 Feb 2012; revised 27 May 2012; accepted 16 Jun 2012; published 19 Jun 2012

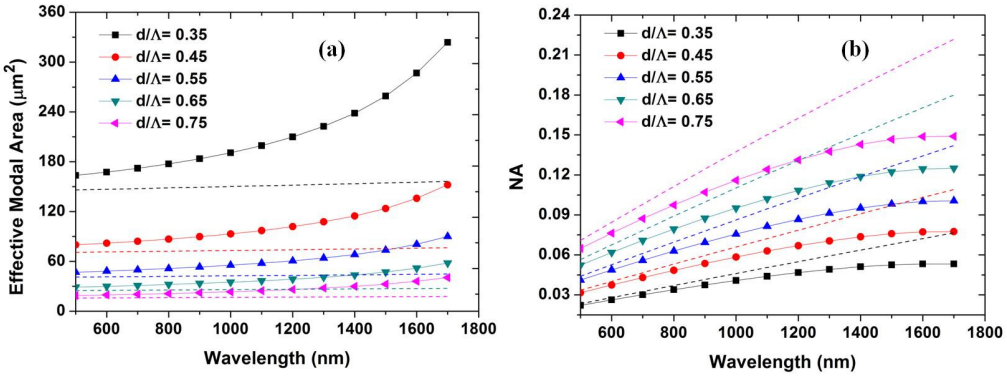

Fig. 8. (a) Effective modal area of the hybrid PCF (solid line) and (b) numerical aperture of the hybrid polymer/Silica PCF with varying relative hole size. The dashed lines correspond to the conventional air-filled PCF.

Finally, we have calculated how the evanescent field changes due to the infusion of PDMS. As expected, the infiltration of a polymer into the holes of a PCF substantially increases the light-matter interaction, thus enhancing the evanescent field. Figure 9 shows the calculated percentage of energy in the PDMS-filled holes for a particular fiber mode (fundamental guiding mode in our case). This is calculated by integrating the optical power inside the PCF holes and dividing it by the total power carried by that mode as expressed in [39]:

$$fraction\ of\ \ power = \frac{\int_{holes} \mathrm{Re}(E_x H_y^* - E_y H_x^*)dxdy}{\int_{Total} \mathrm{Re}(E_x H_y^* - E_y H_x^*)dxdy} \times 100 \qquad (4)$$

In Eq. (4), *Ex*, *Ey* and *Hx*, *Hy* are the respective transverse electric and magnetic fields of the fundamental guiding mode. As the d/Λ increases the interaction of the light with polymer becomes stronger and the fraction of power in the holes of the PCF can be as high as ~13% at 1700 nm. It should be noted that in case of the conventional unfilled PCFs, the fraction of power in the air-holes is negligible for all d/Λ structures.

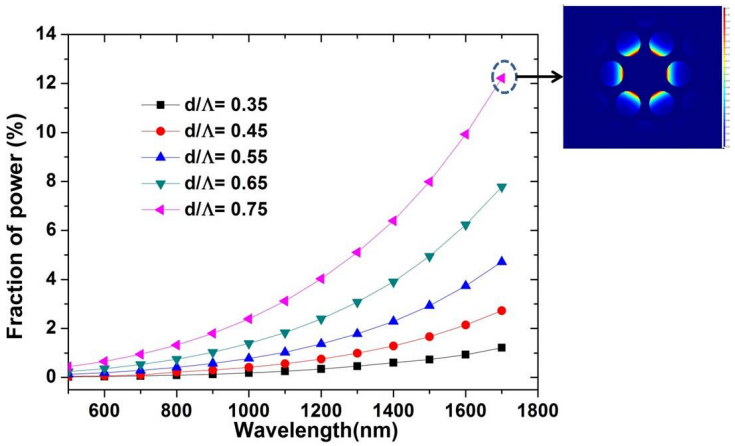

Fig. 9. Fraction of power in the PDMS-filled holes of the PCF versus wavelength for different relative hole sizes. Right inset represents a graphical representation of the evanescent field for the case of d/Λ = 0.75 at 1700 nm wavelength.

#162526 - $15.00 USD Received 8 Feb 2012; revised 27 May 2012; accepted 16 Jun 2012; published 19 Jun 2012

3.2 Thermal properties of the polymer-infused PCF

In this section, we present the thermal properties of the hybrid PDMS infused PCF. All calculations were performed at 633 nm, where PDMS exhibits relative low absorption as well as at 1550nm, which is a widely used wavelength. PDMS exhibit a unique capability to operate over a wide range of wavelengths as compared with polymer or liquids, bearing a potential for developing thermally tune fiber devices (i.e. sensors). In our calculations, the thermo-optic coefficient of PDMS was set to $dn/dT = -4.5\times10^{-4}$/ °C [15], while it was neglected for silica. This is because the thermo-optic coefficient as well as any thermal effect induced is insignificant for low temperatures as high as 100°C [40]. To this end, based on the thermally induced change of the refractive index of PDMS, we calculated the corresponding effective indices of the fundamental guiding mode. Figures 10(a) and 10(b) show the effective index difference (Δn) defined as the difference of the effective indices between the initial (T_0 = 0°C) and actual temperature (x-axis) at 633 and 1550 nm, respectively. From Fig. 10(a), it can be seen, that the change of the effective refractive index with temperature is limited due to the high confinement of the fundamental mode at 633nm. For $d/\Lambda = 0.75$, the difference in the effective indices reaches a maximum of ~2.4×10^{-4} at 100°C. For the same structure at l550nm, the change of the effective index can be as high as 30×10^{-4} (see Fig. 10(b)). This is due to the large overlap between the guiding mode and PDMS-filled cladding providing a significantly capability for designing thermally tuned devices at 1550nm. Figures 10(c) and 10(d) show the unique feature to tune the V-parameter by varying temperature. Figure 10(c) shows the change of the V-parameter at 633 nm, over which the effect is not very strong due to the high confinement of the mode at short wavelengths. In contrast, at 1550nm wavelength, the effect is much stronger as shown in Fig. 10(d).

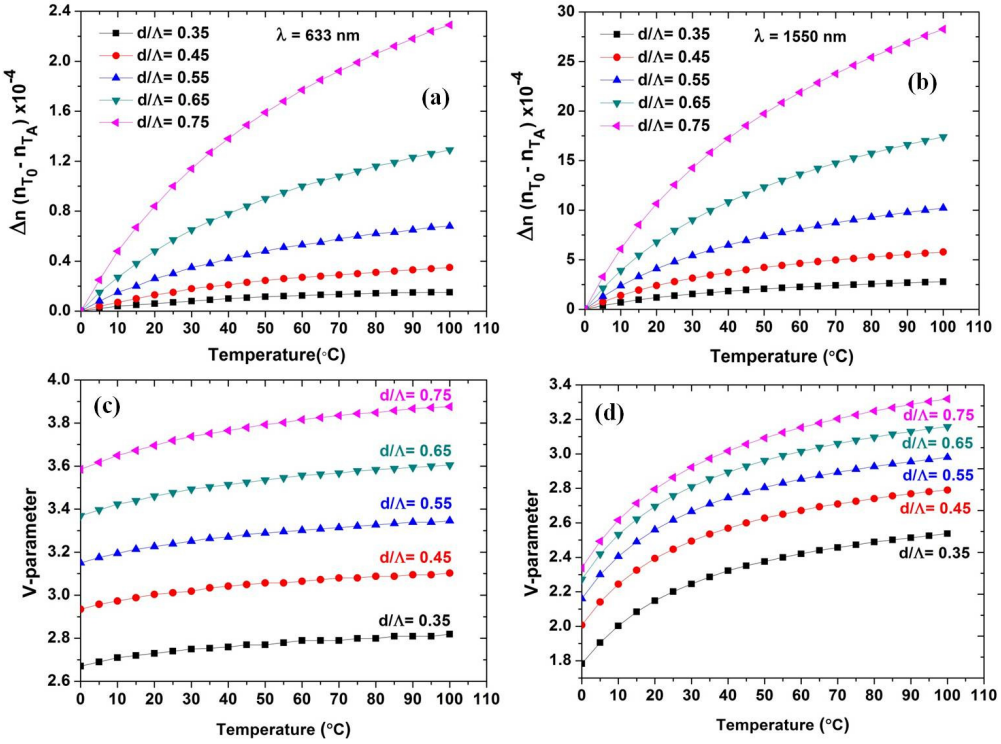

Fig. 10. Effective index difference variation, Δn of the polymer-filled PCF for different relative hole sizes versus temperature at (a) 633nm and (b) 1550 nm. Single-mode operation cut-off (V-parameter) for different temperatures at (c) 633 and (d) 1550nm wavelength.

#162526 - $15.00 USD Received 8 Feb 2012; revised 27 May 2012; accepted 16 Jun 2012; published 19 Jun 2012

Figure 11 displays the corresponding confinement loss variation only for 1550nm, since at 633 is insignificantly small. In general the increase of temperature induces an increase in the refractive index contrast between cladding and core also increases, allowing the fundamental guiding mode to be highly confined to the core of the fiber. From Fig. 11, it can be seen that for relative hole sizes greater than 0.55, the confinement loss is significantly reduced starting from 0.01 dB/m at 0°C to less than $1x10^{-8}$ at 70°C. In contrast for $d/\Lambda = 0.45$ και 0.35, confinement loss reduces more smoothly, starting from a high value of 10dB/m (see $d/\Lambda = 0.35$ curve) to only $1x10^{-4}$ at 100°C (see $d/\Lambda = 0.45$ curve).

In Fig. 12, we show how the thermo-optic effect can tune the EMA and NA of the fiber at both 633 and 1550 nm wavelength for different d/Λ. It can be clearly seen that the variation of EMA in the case of 633nm is very small as compared to 1550nm. At longer wavelengths, i.e. 1550nm, there is efficient interaction between the core mode field and the active material infused into the air-holes and thus for the best case scenario (see Fig. 12(b), $d/\Lambda = 0.35$ curve), EMA can be as high as $400\mu m^2$ and as low as $200\mu m^2$ for a temperature variation of 100°C.

Figures 12(c) and 12(d) display the corresponding NA variation with temperature. As previously mentioned, the change of NA with temperature is directly linked to EMA; therefore at short wavelengths (i.e. 633 nm) the variation of NA is small (see Fig. 12(c)), while at 1550nm NA notably increases with temperature. For example, for the case of $d/\Lambda = 0.75$, NA increases from 0.12 to 0.18 for a 100°C temperature increase. It should be noted here again that for a conventional unfilled PCF, temperature changes do not affect EMA and NA due to very low thermo-optic coefficient of silica. Tuning EMA and NA with temperature is an important feature especially as for example collecting light from non-linear fiber, alleviating the need for fiber post processing.

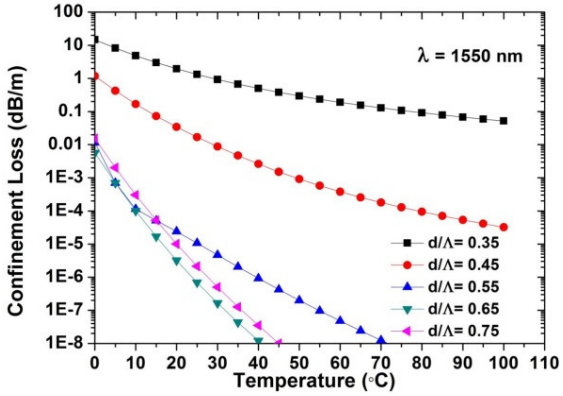

Fig. 11. Confinement loss of the hybrid PDMS infused PCF for different relative hole sizes at 1550 nm.

#162526 - $15.00 USD Received 8 Feb 2012; revised 27 May 2012; accepted 16 Jun 2012; published 19 Jun 2012

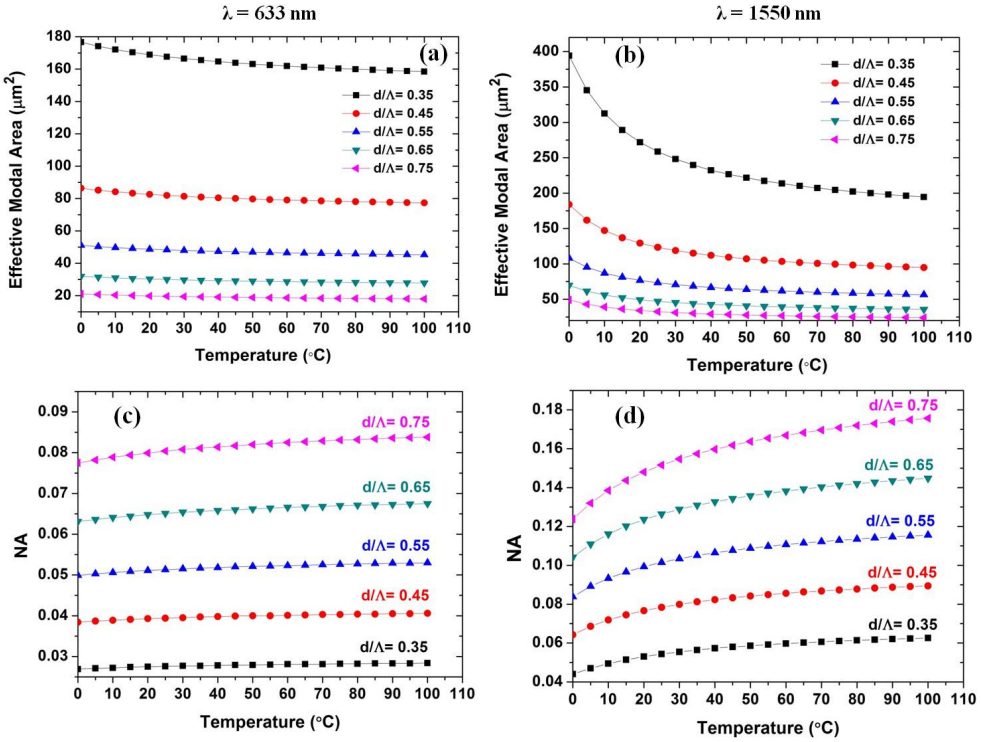

Fig. 12. Effective modal area (EMA) and numerical aperture (NA) variation versus temperature at (a),(c) 633 nm and (b),(d) 1550nm.

Figures 13(a)–13(f) displays the a graphical representation (logarithmic scale) of the fundamental guiding mode at 0°C, 20°C, 40°C, 60°C, 80°C and 100°C. It can be seen that when increasing the temperature, the refractive index contrast between cladding and core increases as well, this is due to the high thermo-optic effect caused of infused PDMS, confining the fundamental guiding mode into to the core of the fiber. Consequently, both EMA and NA are tuned as shown in Fig. 12.

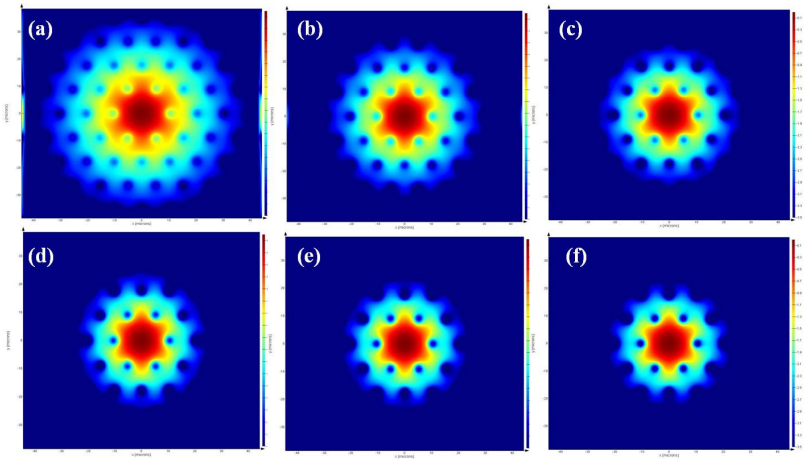

Fig. 13. (a) Single-frame(one per 20°C) excerpts from the simulation video illustrating the tuning of the modal area of the fundament mode of the hybrid polymer/silica PCF with d/Λ = 0.35 at 1550 nm starting from 0°C to 100°C. Subplot (a) corresponds to 0°C and (f) to 100°C (logarithmic scale) (Media 1).

#162526 - $15.00 USD Received 8 Feb 2012; revised 27 May 2012; accepted 16 Jun 2012; published 19 Jun 2012

Finally, we have also calculated, the fraction of power (%) inside the PDMS-filled cladding for different relative hole sizes from 0°C to 100°C. At 633 nm, the high confinement of the mode allows limited interaction with the cladding and thus the fraction of power varies from around 0.1 to 1.25% as shown in Fig. 14(a). However, the same effect is much stronger at 1550 nm and from Fig. 14(b), it can be seen that the fraction of power in the PDMS infused holes spans from 2% to 16% at 0°C for the different relative holes sizes.

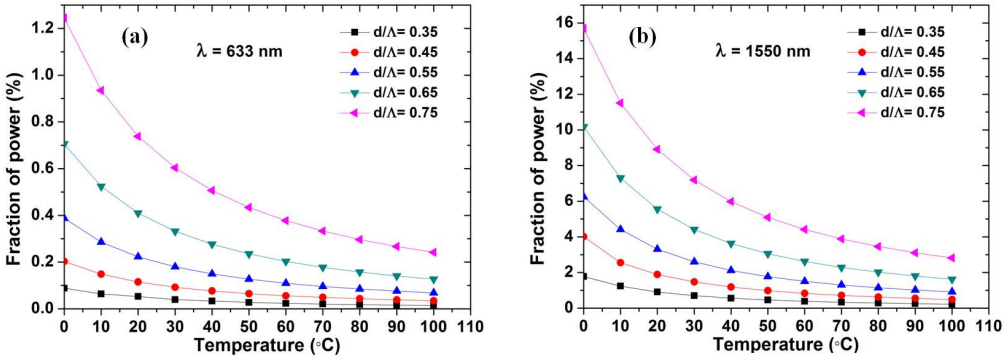

Fig. 14. Fraction of power in the cladding of the hybrid polymer/silica PCF at (a) 633 nm and (B) 1550 nm from 0°C to 100°C.

4. Conclusions

In this paper, the guiding and thermal characteristics of a hybrid polymer (PDMS)/silica photonic crystal fiber were presented. The study was focused on its fundamental characteristics such as the effective index of the fundamental mode, confinement loss, V-parameter, effective modal area (EMA), numerical aperture and the evanescent field of the waveguide for different relative hole sizes (d/Λ = 0.35, 0.45, 0.55, 0.65, 0.75), over 500nm to 1700nm wavelength range. Furthermore, it was also investigated how these parameters can be thermally manipulated over a wide range of temperatures. It was shown that the infusion of PDMS in a conventional PCF allows tuning of these parameters with temperature lending some important features as for example conversion of a multimode to endlessly single mode fiber, tuning EMA and NA of conventional fibers or enhancing evanescent filed interaction. To this end, we may argue that such PDMS (or other featured polymers)-infused PCFs may be used in designing tunable devices i.e. filters, sensors, tunable birefringent devices, etc.

Acknowledgments

This work was supported by the Greek NSRF Program with Grant No. 09SYN-24-769 and European Defense Agency (EDA) with Grant No A-0931-RT. Authors would like to thank Dr. G. Mousdis for his support with the absorption measurements.

#162526 - $15.00 USD Received 8 Feb 2012; revised 27 May 2012; accepted 16 Jun 2012; published 19 Jun 2012